Materials Physics and Mechanics 44 (2020) 221-228 Received: March 2, 2020

STRESS-STRAIN HYSTERESIS SHAPE ESTIMATION OF DIFFERENT SOILS USING DEFORMATION-HISTORY INTEGRAL (DHI) MODEL

A. Vatanshenas[1*], T. Mori[2], M.S. Farhadi[1], T. Länsivaara[1]

[1]Faculty of Built Environment, Tampere University, Finland

[2]Seismic Isolation and Vibration Control Products Development Department, Bridgestone Corporation, Japan

*e-mail: ali.vatanshenas@tuni.fi

Abstract. Different soils show different nonlinear stress-strain patterns. Hence, it is difficult to come up with a general model to predict these shapes. This study investigated the suitability of the DHI model which was not originally formulated for geomaterials. This model was applied to different loading cycles of various types of soils and the model's variables were optimized using nonlinear generalized reduced gradient (GRG) method. Up to five hysteresis springs were considered in the study. The computed error criteria indicated that the DHI model approximated the nonlinear hysteresis shapes appropriately and using three hysteresis springs presented the best estimation for almost all cases. In addition, this model approximated the initial loading cycles better than the final ones.

Keywords: cyclic direct simple shear (CDSS) test, DHI model, dynamic loading, nonlinear plasticity, optimization, soil modeling

1. Introduction

Soil is one of the most problematic materials in terms of material modeling. Surprisingly observations of cyclic shear stress-shear strain responses of soft sensitive clays that their characteristics have been formed by physical and chemical actions over the centuries showed many similarities to a special modern type of elements used in the earthquake engineering field called high damping rubber bearings (HDRB). Recent innovative formulations used for constitutive modeling of these highly nonlinear elements made authors interested to investigate this similarity with more depth. The similarity reveals from two observations: first, hysteresis plots of HDRB and soils show analogous shapes under dynamic loading (Fig. 1) [1-2]. second, stiffness degradation graphs related to soft sensitive clays and HDRB presented in Fig. 2, show similar variation trends [3-4].

Soil nonlinearity is one of the main accomplishments in soil science [5]. However, due to coupling effects of many parameters and microstructural changes after passing a certain strain threshold [6], considering nonlinearity in soil models has been a challenge. In addition, including complexities to the soil model usually end up introducing more parameters that limit its usage in practice [7]. Soil nonlinearity in geotechnics is usually considered via shear stiffness decaying trend and hyperbolic formulas proposed by [8-10]. Nevertheless, it is worthy to investigate what techniques researchers in other fields like earthquake engineering use to consider nonlinearity.

As shown in Fig. 3, DHI model captures different kinds of hysteresis shapes within a single constitutive model [11]. As a result, it can be beneficial for dynamic problems like wind turbines [12-15], where flexibility in stress-strain modeling is advantageous. Extensive studies in the literature have focused on investigating cohesive soil responses under dynamic

http://dx.doi.org/10.18720/MPM.4422020_6

loadings within work-hardening elasto-plasticity concept [16-18]. However, most of the introduced models are quite complicated. Therefore, the main goal of this paper has been applying a simple but robust model that captures the complex nonlinear plasticity within a well-defined constitutive framework. DHI model considers nonlinear plasticity via a relatively simple mathematical framework. This model was mainly introduced for HDRB but it shows no restriction to be implemented for other types of materials.

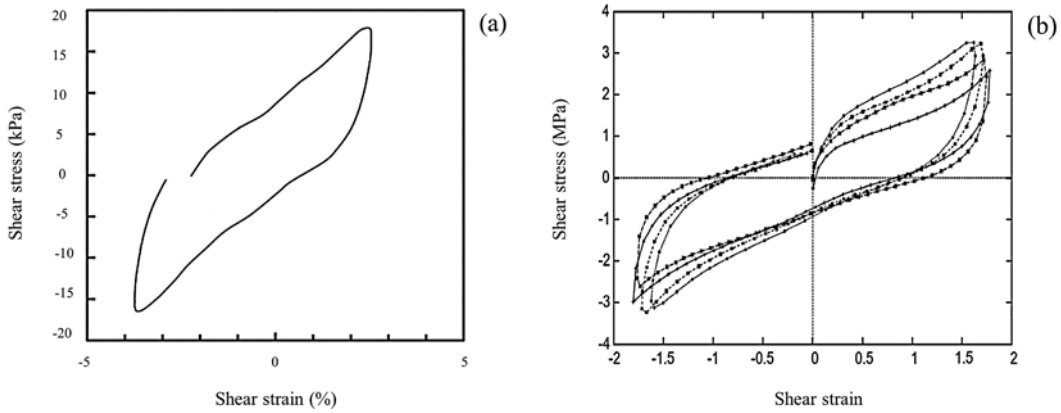

Fig. 1. Comparison of hysteresis trend between fine-grained geomaterial (a) and HDRB (b), modified from [1-2]

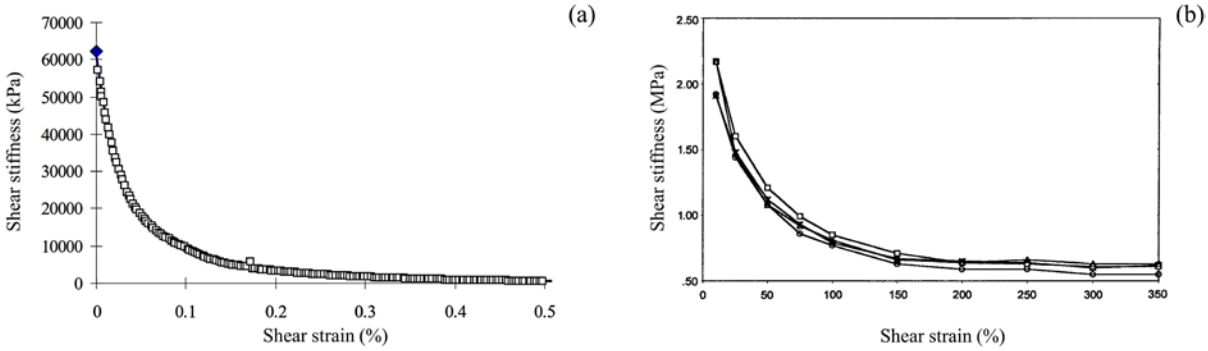

Fig. 2. Comparison of stiffness degradation trend between soft sensitive clay (a) and HDRB (b), modified from [3-4]

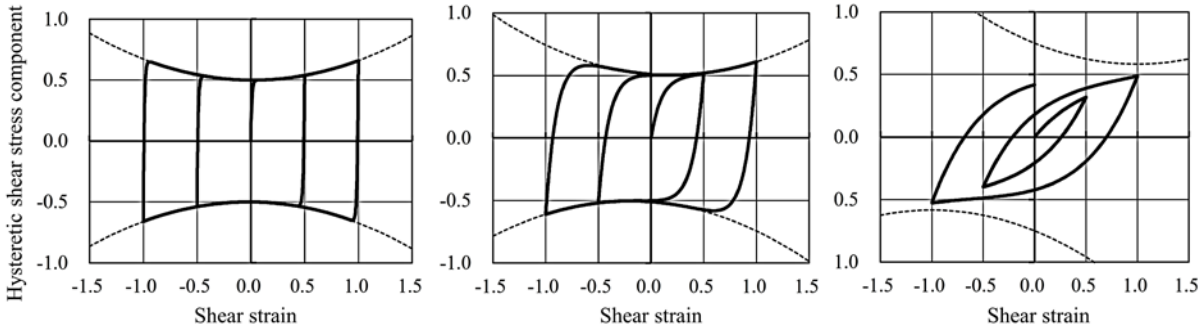

Fig. 3. Various shapes of stress-strain relations covered by DHI model, modified from [11]

2. Formulation of DHI Model

In this section, formulation development of DHI model that has been recently implemented in finite element programs SAP2000 and ETABS, is presented according to former studies in the literature [11,19-23]. DHI model was developed based on hysteresis geometry. It was introduced as a modified version of Simo's viscoelastic model (Eq. 1) [24]. Where S is the second Piola-Kirchhoff stress, W_{vol} volumetric part of elastic stored energy function, $\bar{W}_{dev}$

deviatoric part of elastic stored energy, C right Cauchy-Green tensor, g_n parameter which governs the magnitude of energy dissipation, $\bar{W}_0$ strain energy density function for deviatoric deformation related to viscosity, τ_n relaxation time of nth viscoelastic element and N are the number of nonlinear elasto-plastic springs. Difference between DHI and Simo's model originates from changing time parameter t with the curvilinear integral Γ along the deformation orbit on shear strain plane Υ_x-Υ_y (Eq. 2), where D' is the deviatoric part of deformation rate tensor. Modified equation is presented in (Eq. 3). Where L is the length of curvature in shear strain plane and L_n is relaxation of Γ of nth elasto-plastic spring. Note that by replacing Γ with t domain also changed from (0,t) to (0,L).

$$S = 2\frac{\partial \mathrm{W}_{vol}}{\partial \mathrm{C}} + 2\frac{\partial \bar{W}_{dev}}{\partial \mathrm{C}} + 2\sum_{n=1}^{N} g_n \int_0^t \frac{d}{dt'}\left(\frac{\partial \bar{W}_0}{\partial \mathrm{C}}\right) e^{\frac{-(t-t')}{\tau_n}}\, dt', \tag{1}$$

$$\Gamma = \int_0^t \sqrt{\frac{2}{3} D' : D'}\, dt\ , \tag{2}$$

$$S = 2\frac{\partial \mathrm{W}_{vol}}{\partial \mathrm{C}} + 2\frac{\partial \bar{W}_{dev}}{\partial \mathrm{C}} + 2\sum_{n=1}^{N} g_n \int_0^L \frac{d}{d\Gamma'}\left(\frac{\partial \bar{W}_0}{\partial \mathrm{C}}\right) e^{\frac{-(\Gamma-\Gamma')}{L_n}}\, d\Gamma'\ . \tag{3}$$

By taking elastic deviatoric stiffness degradation into account (Eq. 4) was obtained, in which Ξ is the damage function. This constitutive relation was formulated in six degrees of freedom. Therefore, this relation was rearranged in such a way to be applicable as bi-directional shear deformation analytical model for time history analysis (Eq. 5). Where τ^{e} and τ^{h} are elasticity and hysteretic part of total shear stress. In addition, as shown in Fig. 4, elasto-plasticity region was introduced as n hysteretic parts to model nonlinear plasticity.

$$S = 2\frac{\partial \mathrm{W}_{vol}}{\partial \mathrm{C}} + 2\,\Xi\,\frac{\partial \bar{W}_{dev}}{\partial \mathrm{C}} + 2\sum_{n=1}^{N} g_n \int_0^L \frac{d}{d\Gamma'}\left(\frac{\partial \bar{W}_0}{\partial \mathrm{C}}\right) e^{\frac{-(\Gamma-\Gamma')}{L_n}}\, d\Gamma', \tag{4}$$

$$\tau = \tau^{\mathrm{e}} + \sum_{n=1}^{N} [\tau^{\mathrm{h}}]_n\ . \tag{5}$$

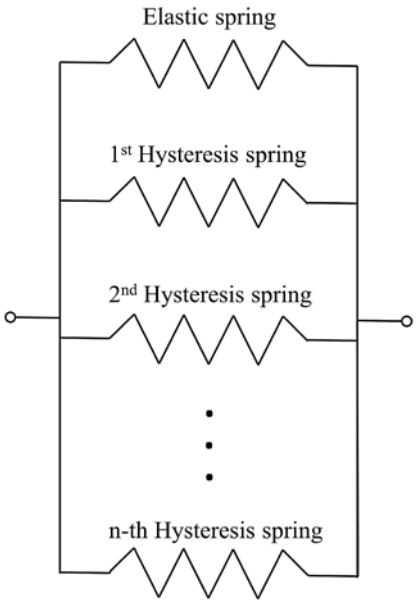

Fig. 4. Schematic of DHI model

Overall, after some more calculations, generalized formulation for the mth strain reversal for unidirectional loading takes the form of (Eq. 6) in which $\Upsilon_r{}^{(m)}$ is the loading/unloading strain. $\bar{\tau}_n$ and $\bar{\Upsilon}_n$ are control shear and control strain that govern hysteretic behavior and size of energy absorption by nth hysteretic spring, respectively (Fig. 5). Note that this final form of

proposed formulation only requires $2n$ input parameters ($\bar{\tau}_n$ and $\bar{Y}_n$) for elasto-plasticity region, where n is the number of hysteretic springs.

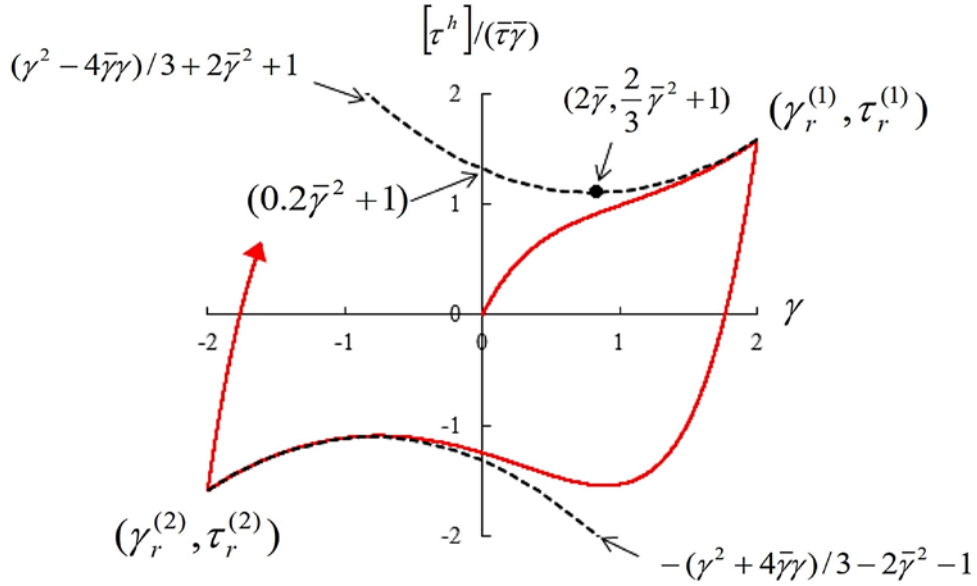

Fig. 5. Hysteresis shape with geometric nonlinearity [11]

$$\tau = \tau^{e} + \sum_{n=1}^{N} \bar{\tau}_n \bar{Y}_n \left[\frac{sign(\Delta Y)-4\bar{Y}_n Y}{3} + sign(\Delta Y)\left(2\bar{Y}_n{}^2+1\right) - \left(\frac{2}{3}\left(\bar{Y}_n - \text{sign}\left(Y_r{}^{(m)}\right)\right)(Y + 3sign(\Delta Y)\bar{Y}_n) - \text{sign}(\Delta Y)\left(1+\bar{Y}_n{}^{(m)2}\right) + \frac{[\tau^{h(m-1)}]_n}{\bar{\tau}_n \bar{Y}_n}\Big|_{Y=Y_r{}^{(m)}}\right)\right] e^{\frac{Y-Y_r{}^{(m)}}{\bar{Y}_n}} . \quad (6)$$

3. Hysteresis Patterns Estimation

CDSS test was considered in this study to evaluate lateral hysteresis patterns of different geomaterials. DHI model was applied to estimate the stress-strain curves for different types of soils including silt, sand, clay, and tailings under different cycles of loading available in the literature [1]. The estimations were repeated for one to five hysteresis springs considered in the model. Model parameters were chosen using generalized reduced gradient (GRG) method. Both Mean Square Error (MSE) and coefficient of determination (R^2) for each series of computations were derived. The results are presented in Table 1. Considering different numbers of springs, it was revealed that for almost all cases, three springs led to the desired results. Increasing the number of springs and using four and five springs did not improve the stress-strain estimations considerably. Increasing the accuracy by involving more springs to the model is illustrated in Fig. 6, for the Fraser River silt under 10^{th} cycle of loading. In almost all cases, the model estimated better in initial cycles of loading because much less irregularities in term of hysteretic shape occur in initial cycles. For instance, the error criteria for Fraser River silt for 2^{nd} cycle were better than the same results for 10^{th} cycle. In addition, the observed irregularities and hardening behavior for higher number of cycles in the CDSS tests, might be due to some constraint problems used for the experiments.

Although the measured versus estimated stress-strain curves were good according to the R^2 criterion, the stress-strain curves were also plotted to enable the engineer to judge visually. The curves derived out of using three springs are illustrated in Fig. 7, for all the considered soil types in this study for both early and final stages of loading. It was observed that some estimations were not as satisfactory as expected; although, the error criteria had shown some

good quantities of error. It can be seen for some cases like River sand type I (4th cycle) and Laterite tailings (6th cycle).

Table 1. Evaluating model accuracy by MSE and R^2 criteria

Soil type	Cycle No.	MSE					R^2				
		1 spring	2 springs	3 springs	4 springs	5 springs	1 spring	2 springs	3 springs	4 springs	5 springs
Fraser River silt	2	1.780	0.558	0.282	0.282	0.281	0.995	0.997	0.998	0.998	0.998
Fraser River silt	10	6.454	2.076	1.315	1.190	0.922	0.965	0.991	0.993	0.994	0.995
River Sand Type I	2	1.454	1.306	1.260	0.573	0.511	0.995	0.995	0.997	0.997	0.997
River Sand Type I	4	10.415	3.635	3.641	3.638	3.605	0.915	0.970	0.970	0.970	0.970
Kitimat clay	1	9.970	4.293	2.355	2.418	2.368	0.989	0.986	0.992	0.992	0.992
Kitimat clay	10	4.957	2.967	2.964	2.176	2.165	0.982	0.992	0.992	0.993	0.994
Laterite tailings	1	11.747	6.275	5.703	5.703	5.703	0.991	0.992	0.994	0.994	0.994
Laterite tailings	6	14.570	6.079	3.894	3.870	3.675	0.945	0.981	0.986	0.986	0.987

Regardless of all the positive advantages of the discussed model, it also has minor drawbacks that shows there is room for enhancement. For instance, the discussed model focuses on hysteresis response and neglects the development of pore water pressure. In addition, DHI model does not consider stiffness degradation per cycle as the loading continues but has the potential to be upgraded using other models like Pivot model [25]. Pivot model is a multi-linear plastic model that is also formulated based on geometry that makes it easier to be added to the DHI model to overcome this drawback.

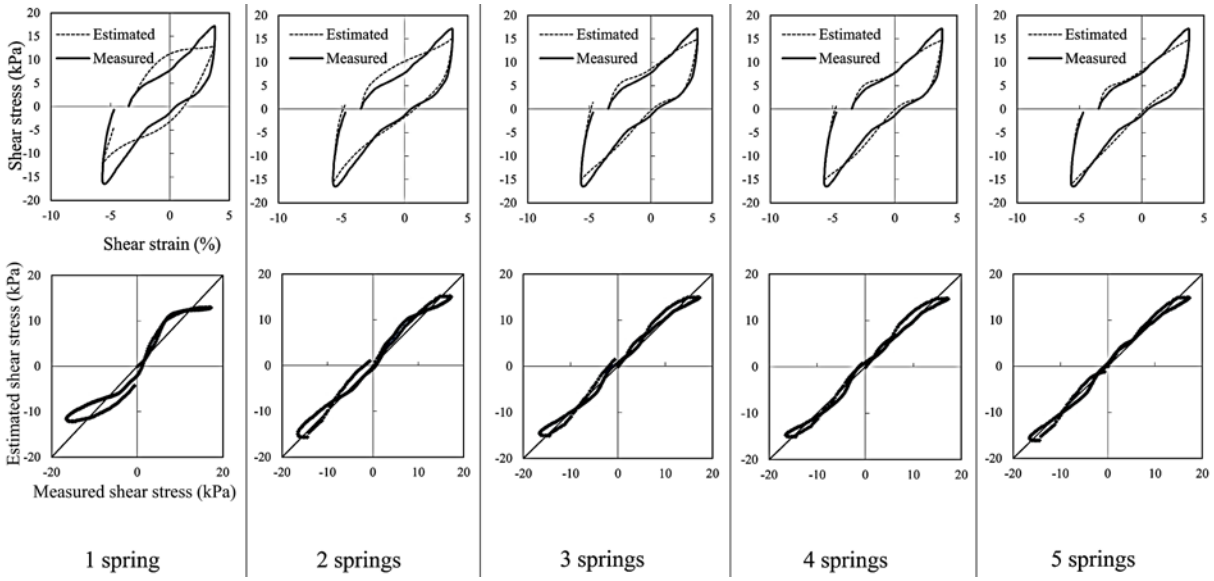

Fig. 6. Estimated versus measured shear stress for different number of springs in DHI model for Fraser River silt, extracted from [1]

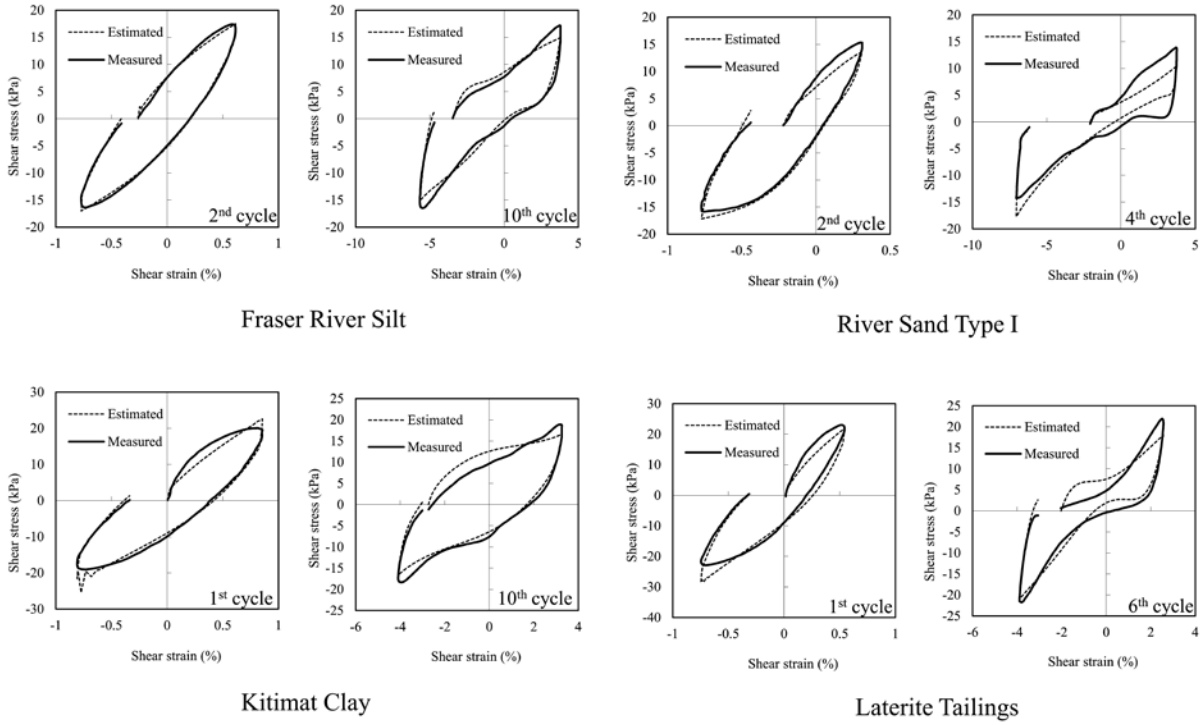

Fig. 7. Comparison of model estimations with experimental results for different soils, extracted from [1]

6. Conclusions

Main objective of this paper was to open new insights into soil modeling field by showing potential of implementing new techniques in material science for soils. Flexibility of DHI model to predict nonlinear plasticity within a simple innovative mathematical framework was discussed in this study. Soil's irregular hysteresis shapes were estimated via DHI model that was not mainly formulated for soils. DHI model showed adequate results to approximate stress-strain curves of various types of soils including silt, sand, clay, and tailings under cyclic lateral loading. Due to less shape complexities, DHI model estimated early stages of loading better than the final ones. It was also observed that three hysteresis springs ended up with the suitable results and increasing number of springs after that did not affect the results significantly. Merging DHI model with other models like pivot model to capture stiffness degradation per each cycle and finding correlations between model parameters with soil index properties using adequate number of experimental data are suggested for future studies.

Acknowledgements. *The authors acknowledge financial support from Tampere University. Moreover, we would like to offer our special thanks to Dr. Nobuo Murota from Bridgestone Corporation for his sincere efforts to clarify the DHI model.*

References

[1] Wijewickreme D, Soysa A. Stress–strain pattern–based criterion to assess cyclic shear resistance of soil from laboratory element tests. *Canadian Geotechnical Journal*. 2016;53(9): 1460-1473.

[2] Bhuiyan AR, Okui Y, Mitamura H, Imai T. A rheology model of high damping rubber bearings for seismic analysis: Identification of nonlinear viscosity. *International Journal of Solids and Structures*. 2009;46(7-8): 1778-1792.

[3] Länsivaara T. *A study of the mechanical behavior of soft clay. Dissertatioon*. Norwegian University of Science and Technology: Norway; 1999.

[4] Naeim F, Kelly JM. *Design of seismic isolated structures: from theory to practice.* John Wiley & Sons; 1999.
[5] Atkinson JH. Non-linear soil stiffness in routine design. *Géotechnique*. 2000;50(5): 487-508.
[6] Vucetic M. Cyclic threshold shear strains in soils. *Journal of Geotechnical engineering*. 1994;120(12): 2208-2228.
[7] Brinkgreve RB. Selection of soil models and parameters for geotechnical engineering application. In: *InSoil constitutive models: Evaluation, selection, and calibration*; 2005. p.69-98.
[8] Kondner RL. Hyperbolic stress-strain response: cohesive soils. *Journal of the Soil Mechanics and Foundations Division*. 1963;89(1): 115-44.
[9] Hardin BO, Drnevich VP. Shear modulus and damping in soils: design equations and curves. *Journal of the Soil Mechanics and Foundations Division*. 1972;98(sm7): 667-692.
[10] Ramberg W, Osgood WR. *Description of stress-strain curves by three parameters*. 1943.
[11] Kasai K, Mori T, Masaki N, Murota N. Simplified Modeling for Two-Directional Behavior of High Damping Rubber Isolation Bearings. In: *Proc. 11th U.S. National Conference on Earthquake Engineering*. 2018.
[12] Kaynia AM. Seismic considerations in design of offshore wind turbines. *Soil Dynamics and Earthquake Engineering*. 2019;124: 399-407.
[13] Skau KS, Page AM, Kaynia AM, Løvholt F, Norén-Cosgriff K, Sturm H, Andersen HS, Nygard TA, Jostad HP, Eiksund G, Havmøller O. REDWIN–REDucing cost in offshore WINd by integrated structural and geotechnical design. *InJournal of Physics: Conference Series*. 2018;1104(1): 012029.
[14] Katsanos EI, Thöns S, Georgakis CT. Wind turbines and seismic hazard: a state of the art review. *Wind Energy*. 2016;19(11): 2113-2133.
[15] Damgaard M, Zania V, Andersen LV, Ibsen LB. Effects of soil–structure interaction on real time dynamic response of offshore wind turbines on monopiles. *Engineering Structures*. 2014;75: 388-401.
[16] Frydman S, Talesnick M, Almagor G, Wiseman G. Simple shear testing for the study of the earthquake response of clay from the Israeli continental slope. *Marine Georesources & Geotechnology*. 1988;7(3): 143-71.
[17] Pande GN, Pietruszczak S. A critical look at constitutive models for soils. *Geomechanical modelling in engineering practice*. 1986: 369-395.
[18] PreÂvost JH. Modelling the cyclic stress-strain response. In: O'Reilly MP, Brown S. (eds.) *Cyclic loading of soils: from theory to design.* The Netherlands: Van Nostrand Reinhold; 1991. p.19-69.
[19] Kato H, Mori T, Murota N, Suzuki S, Kikuchi M. A new hysteresis model based on an integral type deformation-history for elastomeric seismic isolation bearings. In: *15th World Conferences on Earthquake Engineering (WCEE)*. 2012.
[20] Mori T, Kato H, Nakamura M, Masaki N, Murota N, Kasai K. Hysteresis model of deformation-history integral type for Isolators. In: *Proceedings of the 5th Asian Conference on Earthquake Engineering (ACEE)*. 2014.
[21] Kato H, Mori T, Murota N, Kikuchi M. Analytical model for elastoplastic and creep-like behavior of high-damping rubber bearings. *Journal of Structural Engineering*. 2014;141(9): 04014213.
[22] Masaki N, Mori T, Murota N, Kasai K. Validation of Hysteresis Model of Deformation-History Integral Type for High Damping Rubber Bearings. In: *Proceedings of the 16th World Conference on Earthquake Engineering (WCEE)*. 2017.
[23] Computers and Structures, Inc. Technical note, high-damping rubber isolator link property. 2017.

[24] Simo JC. On a fully three-dimensional finite-strain viscoelastic damage model: formulation and computational aspects. *Computer methods in applied mechanics and engineering*. 1987;60(2): 153-73.
[25] Dowell OK, Seible F, Wilson EL. Pivot hysteresis model for reinforced concrete members. *ACI Structural Journal*. 1998;95: 607-17.